Statistical Analysis For FEM EEG Source Localization in Realistic Head Models

Leonid Zhukov, David Weinstein and Chris Johnson

Email: zhukov@cs.utah.edu, dmw@cs.utah.edu, crj@cs.utah.edu

UUCS-2000-003

Center for Scientific Computing and Imaging
Department of Computer Science
University of Utah
Salt Lake City, UT 84112 USA

February 1, 2000

Abstract

Estimating the location and distribution of electric current sources within the brain from electroencephalographic (EEG) recordings is an ill-posed inverse problem. The ill-posed nature of the inverse EEG problem is due to the lack of a unique solution such that different configurations of sources can generate identical external electric fields.

In this paper we consider a spatio-temporal model, taking advantage of the entire EEG time series to reduce the extent of the configuration space we must evaluate. We apply the recently derived *infomax* algorithm for performing Independent Component Analysis (ICA) on the time-dependent EEG data. This algorithm separates multichannel EEG data into activation maps due to temporally independent stationary sources. For every activation map we perform a source localization procedure, looking only for a single dipole per map, thus dramatically reducing the search complexity. An added benefit of our ICA preprocessing step is that we obtain an *a priori* estimation of the number of independent sources producing the measured signal.

INTRODUCTION

Electroencephalography (EEG) is a technique for the non-invasive characterization of brain function. Scalp electric potential distributions are a direct consequence of internal electric currents associated with neurons firing and can be measured at discrete recording sites on the scalp surface over a period of time.

Estimation of the location and distribution of current sources within the brain from the potential recording on the scalp (*i.e.,* source localization) requires the solution of an inverse problem. This problem is ill-posed in the Hadamard sense; specifically, its solution is not necessarily unique. Physically, this is a consequence of the linear superposition of the electric field. Specifically, different internal source configurations can provide identical external electromagnetic fields. Additionally, only a finite number of measurement of scalp potential are available, increasing the ill-posedness of the problem.

There exist several different approaches to solving the source localization problem. Initially, most of these were implemented on a non-realistic spherical model of the head. Those methods which proved promising were then extended to work on realistic geometry. One of the most general methods involves starting from some initial distributed estimate of the source and then recursively enhancing the strength of some of the solution elements, while decreasing the strength of the rest of the solution elements until they become zero. In the end, only a small number of elements will remain nonzero, yielding a localized solution. This method is implemented, for example, in the FOCUSS algorithm [Gorodnitsky, 1995].

Another approach incorporates *a priori* assumptions about sources and their locations in the model. Electric current dipoles are usually used as sources, provided that the regions of activations are relatively focused [Nunez, 1981]. Although a single dipole model is the most widely used model, it has been demonstrated that a multiple dipole model is required to account for a complex field distribution on the surface of the head [Supek, 1993].

Finally, there is a group of algorithms that utilize a time course of dipole activations. Here, rather than fit the assumed dipoles on an instant-by-instant basis, they are fitted by minimizing the least-square error residual over the the entire evoked potential epoch [Scherg, 1985]. A more advanced approached is developed in the multiple signal characterization algorithm, MUSIC, and in its extension, RAP-MUSIC. These algorithms use principal component subspace projections to find multiple dipole sources [Mosher, 1992].

In this paper we propose a new approach to the problem of source localization for

the inverse EEG problem. Our solution consists of two steps. First, we preprocess the time dependent data, using the Independent Component Analysis (ICA) [Bell, 1995, Amari, 1996] signal processing technique. The result of the preprocessing is a set of time-series signals at each electrode, where each time-series corresponds to an independent source in the model. The number of different maps created by the ICA is equal to the number of temporally independent, stationary sources in the problem. To localize each of these independent sources, we solve a separate source localization problem. Specifically, for each independent component, we choose an instant in time from the signal and employ a downhill simplex search method [Nedler, 1965] to determine the dipole which best accounts for that particular component's contribution of the measured potentials at the electrodes.

In our study we use simulated data obtained by placing dipoles in the brain in positions corresponding to physiologic phenomena. We chose to incorporate three physiologically plausible sources: the first in the temporal lobe (corresponding to an epileptic focus), the second in the occipital lobe (corresponding to observed visual evoked response (ERP) studies), and the third in the frontal lobe (corresponding to language processing). For each of these sources, we used a time signal from a clinical study to define their magnitudes over time. That is, we place the three current dipoles inside our finite element model, and for each instant in time, we project the realistic ERP-length activation signals onto 32 clinically measured scalp electrode positions. The electrode positions are shown in Figure 1. Projecting the sources onto the electrodes requires the solution of a forward problem.

FORWARD PROBLEM

The EEG forward problem can be stated as follows: given position and activations of dipole current sources, and the geometry and electrical conductivity of the different regions within the head, calculate the distribution of the electric potential on the surface of the head (scalp). Mathematically, this problem can be described by Poisson's equation for electrical conduction in the head [Plonsey, 1995]:

$$\nabla \cdot (\sigma \nabla \Phi) = -\sum I_s, \quad \text{in } \Omega \tag{1}$$

and Newman boundary conditions on the scalp

$$\sigma(\nabla \Phi) \cdot \mathbf{n} = 0, \quad \text{on } \Gamma_\Omega, \tag{2}$$

where σ is a conductivity tensor and I_s are the volume currents density due to current dipoles placed within the head. The unknown Φ is the electric potential created in

the head by the distribution of current from the dipole sources. To solve Poisson's equation numerically, we started with the construction of a computational model. The realistic head geometry was obtained from MRI data, where the volume was segmented and each tissue material was labeled in the underlying voxels [Wells, 1994]. The segmented head volume was then tetrahedralized via a mesh generator which preserved the classification when mapping from voxels to elements [Schmidt, 1995]. For each tissue classification, we assigned a conductivity tensor from the literature [Foster, 1989]. A cut-through of the classified mesh is shown in Figure 2. We then used the finite element method (FEM) to compute a solution within the entire volume domain [Jin, 1993]. The FEM has the advantage that we are able to place current sources in any location (not only on the mesh nodes as in the finite difference method) by simply re-tetrahedralizing the surrounding volume with a Watson-style algorithm [Watson, 1981] after inserting the sources. Our head model consisted of approximately 768,000 elements and $N = 164,000$ nodes.

Using FEM we obtain the system of equations

$$\mathbf{A}_{ij}\Phi_j = \mathbf{b}_i, \tag{3}$$

where $\mathbf{A}_{ij}$ is an $N \times N$ stiffness matrix, $\mathbf{b}_i$ is a source vector and Φ_j is vector of unknow potentials on every node. The $\mathbf{A}$ matrix is sparse (approximately 2,000,000 non-zeroes entries), symmetric and positive definite.

The solution of this linear system was computed using a parallel conjugate gradient (CG) method and required approximately 12 seconds of wall-clock time on a 14 processor SGI Power Onyx with 195 MHz MIPS R10000 processors. The solution to a single dipole source forward problem is visualized in Figure 3. In this image, we display an equipotential surface in wire frame, indicate the dipole location with red and blue spheres, cut-through the initial MRI data with orthogonal planes, and render the surface potential map of the bioelectric field on the cropped scalp surface.

In order to obtain time dependent data, we assigned the different time activations described above to the dipoles and computed the resulting projection on all electrodes as a function of time. We considered a 32 electrode model for this study.

The solution of the forward problem is needed not only to derive the simulated electrode recordings, but also later on as the iteratively applied engine for solving the inverse source localization problem.

INVERSE PROBLEM

The general EEG inverse problem can be stated as follows: given a time dependent set of electric potentials on the surface of the head and the associated positions of those measurements, as well as the geometry and conductivity of the different regions within the head, calculate the locations and magnitudes of the electric current sources within the brain. Mathematically, it is an inverse source problem in terms of the primary electric current sources within the brain and can be described by the same Poisson's equation as the forward problem (1), but with a different set of boundary conditions on the scalp:

$$\sigma(\nabla\Phi)\cdot\mathbf{n}=0, \quad \text{and} \quad \Phi=\phi \quad \text{on} \quad \Gamma_\Omega, \tag{4}$$

where ϕ is the electrostatic potential on the surface of the head known at discrete points - electrode locations, and I_s in (1) are now unknown current sources.

The solution to this inverse problem can be formulated as finding a least squares fit of a set of current dipoles to the observed data for a single time step, or minimization with respect to the model parameters of the following cost function:

$$\sqrt{\sum_{j=1}^{32}(\phi_j-\hat{\phi}_j)^2/32}, \tag{5}$$

where ϕ_i is the value of the measured electric potential on the i^{th} electrode and $\hat{\phi}_i$ is the result of the forward model computation for a particular choice of parameters; the sum extends over all channels.

To employ the above method we must solve the forward problem for every possible configuration and number of dipoles. Each dipole in the model has 6 parameters: location coordinates (x, y, z), orientation (θ, ϕ) and time-dependent dipole strength $P(t)$. The number of dipoles is usually determined by iteratively adding one dipole at a time until a "reasonable" fit to the data has been found. Even when restricting the location of the dipole to the lattice sites, the configuration space is factorially large. This is a bottleneck of many localization procedures [Supek, 1993, Harrison, 1996].

Assume now that we have somehow managed to filter the signals on the electrodes, such that we know electrode potentials due to every dipole separately. Then for every set of electrode potentials we need to search only for one dipole, thus dramatically reducing the configuration space. We will discuss this useful filtering technique in the next section.

STATISTICAL PREPROCESSING OF THE DATA: INDEPENDENT COMPONENT ANALYSIS

In EEG experiments, electric potential is measured with an array of electrodes (typically 32/64/128) positioned primarily on the top half of the head, as shown in Figure 1. For studies of the human visual/auditory system (ERP studies), the data are typically sampled every millisecond during the interval of interest after stimulus presentation, and are averaged over many trials to remove background noise. For a given electrode configuration, the time dependent data can be arranged as a matrix, where every column corresponds to the sampled time frame and every row corresponds to a channel (electrode). For example, the data obtained by 32 electrodes in 180 ms can be sampled in 180 frames and represented as a matrix (32×180). Below we will refer to this matrix as $\mathbf{x}(t_k)$, where instead of a continuous variable t we have sampled time frames t_k.

Independent component analysis (ICA) is a statistical method for transforming an observed multidimensional random vector into components that are as independent from each other as possible [Bell, 1995]. The algorithm achieves this by factoring the multivariate probability density function of the input signals into the product of $f_{\mathbf{y}} = \prod_i f_{\mathbf{y_i}}(\mathbf{y_i})$ probability density functions (p.d.f.) of every independent variable. This factorization involves making the mutual information between variables (channels) go to zero, *i.e.*, making output signals that are statistically independent. The ICA process consists of two phases: the learning phase and the processing phase. During the learning phase, the ICA algorithm finds a matrix $\mathbf{W}$, which minimizes the Kullback-Leibler divergence between the multivariate probability density and the marginal distributions (p.d.f) of transformed input vectors $\mathbf{x}(t_k)$ [Amari, 1996]:

$$D(\mathbf{W}) = \int f(\mathbf{y}) log \frac{f(\mathbf{y})}{\prod_i f_i(\mathbf{y}_i)} d\mathbf{y}, \tag{6}$$

where

$$\mathbf{y}(t_k) = \frac{\mathbf{1}}{\mathbf{1} + e^{-\mathbf{W} \cdot \mathbf{x}(t_k)}}. \tag{7}$$

The $\mathbf{W}$ matrix is iteratively adjusted to minimize integral (6) by using the data vectors $\mathbf{x}(t_k)$:

$$\mathbf{W}_{k+1} = \mathbf{W}_k + \mu_k \cdot (\mathbf{I} + (\mathbf{1} - 2 \cdot \mathbf{y}(t_k) \cdot (\mathbf{W}_k \cdot \mathbf{x}(t_k))^T) \cdot \mathbf{W}_k, \tag{8}$$

where μ_k is a learning rate and $\mathbf{I}$ is the identity matrix [Makeig, 1994]. We decrease the learning rate during the iterations and stop when μ_k becomes smaller than 10^{-6}, or in other words, when on consecutive steps the unmixing matrix $\mathbf{W}$ does not change by more than 10^{-6}.

The second phase of the ICA algorithm is the actual source separation. Independent components (activations) can be computed by applying the unmixing matrix $\mathbf{W}$ to the initial data:

$$\mathbf{u}(t_k) = \mathbf{W} \cdot \mathbf{x}(t_k). \tag{9}$$

There are several assumptions one needs to make about the sources in order to use ICA algorithms:

- the sources must be independent (signals come form statistically independent brain processes);
- there is no delay in signal propagation from the sources to detectors (conducting media without delays at source frequencies);
- the mixture is linear (Laplace's equation is linear);
- the number of independent signal sources does not exceed the number of electrodes (we expect to have fewer strong sources than our 32 electrodes).

ICA returns the source activations up to permutation and scale, because it operates on distribution functions, which do not depend on the relative strength or order of the signals (this also means that the relative polarities of the obtained signals are meaningless). After computing the unmixing matrix $\mathbf{W}$, we can separate the independent source signals using (9). Projection of independent activation maps back onto the electrode arrays can be done by:

$$\hat{\mathbf{x}}^i(t_k) = \mathbf{W}_{ki}^{(-1)} \cdot \mathbf{u}_i(t_k), \tag{10}$$

where $\hat{\mathbf{x}}^i(t_k)$ is the set of scalp potentials due to just the i^{th} source.

As such, ICA allows us to reconstruct surface potentials that would exist due to each dipole as if it were the only source. For example, if the output of ICA gives three strong activation channels, that means we will be looking for only three dipoles. Projecting each activation map on the scalp electrodes gives us three different maps, each with a time sequence of values. For each activation map, we choose one value from the time sequence (fixed point in time), and then use each map to localize one dipole using the downhill simplex method. The results of numerical experiments are presented in the next section.

NUMERICAL SIMULATIONS

We prepared the simulated data as described in the previous sections. The time dependent course of 180 ms for all 32 channels is shown in Figure 4. We also provide

a color mapped plot of the potentials on the surface of the head for the time step at 160 ms in Figure 7. As can be seen in this figure, the distribution of potentials on the scalp can hardly be attributed to a single dipole, but rather to a configuration of several dipoles. We perform the ICA procedure on the given time dependent EEG data and the resulting activation maps are shown in Figure 5. Notice that there are only three different activation patterns presented; the rest are either redundant or are essentially noise. Projecting the first activation on all 32 channels, we get the signals shown in Figure 6, which are the potentials due to the single temporal lobe dipole. Plotting the potentials again for the time step at 160 ms in Figure 8, one can easily recognize the surface potential map as resulting from the activation a single dipole source.

We can now check the accuracy of the ICA decomposition by comparing it to the results of the forward problem simulation run with two of the three dipoles "turned off". Because ICA does not preserve scale, we use correlation coefficients as our metric for comparing the potentials at the electrodes. The sets of electrode potentials are viewed as vectors in N-space (in our case of 180 time steps, $N = 180$) and the cosine of the "angle" between them is calculated by taking the dot-product of the two vectors after they've been normalized. For the jth channel, the correlation coefficient will be:

$$CC_j = \frac{\sum_k (\mathbf{x}_j(t_k) \cdot \hat{\mathbf{x}}_j(t_k))}{|\mathbf{x}_j| \cdot |\hat{\mathbf{x}}_j|} \tag{11}$$

A value of $CC_j = 1$ indicates that the simulated and ICA recovered time series at that electrode are identical up to a scaling factor. The ICA error can thus be cumulatively estimated over all electrodes over the entire time sequence, by evaluating the root-mean-square (RMS) difference of CC_j from 1 over all channels:

$$\sqrt{\sum_{j=1}^{32} (CC_j - 1)^2 / 32} \tag{12}$$

Evaluated with the above formula, our three activation projections restored the original (unmixed) potential distribution with RMS errors of 3%, 4% and 10%, respectively.

We then applied the downhill method [Nedler, 1965] to find the minimum of the multidimensional cost function. In an N dimensional space, the simplex is a geometrical figure that consists of N+1 interconnected vertices (for example, in our case we have a 6 dipole parameters, so the simplex has 7 vertices). The downhill simplex method minimizes a function by taking a series of steps, each time moving the point in the simplex away from where the function is largest. Occasionally the method converges to non-physical solutions and must be restarted [Huang, 1996].

The localized temporal lobe dipole was found to be accurate within 7 mm of the actual source. We repeated this localization procedure for the occipital and frontal lobe dipoles and were able to determine their positions with errors of 9 and 16 mm, respectively.

CONCLUSIONS

We have presented an algorithm that reduces the complexity of localizing multiple neural sources by exploiting the time-dependence of the data. We have shown that on a realistic head model with simulated EEG data, our algorithm is capable of correctly predicting the number of independent sources in the model and reconstructing potentials due to each source separately. These potential maps can be successfully used by source localization methods to independently localize separate sources.

References

[Amari, 1996] Amari, S. and Cichocki, A. and Yang, H.H. A new learning algorithm for blind signal separation, *Advances in Neural Information Processing Systems* 8, MIT press, 1996.

[Bell, 1995] Bell, A.J. and Sejnowski, T.J. An information-maximization approach to blind separation and blind deconvolution, *Neural Computation* 7, 1129-1159, 1995.

[Foster, 1989] Foster, K.R. and Schwan, H.P. Dielectric properties of tissues and biological materials: A critical review, *Critical Reviews in Biomed. Eng.* 17, 25-104, 1989.

[Gorodnitsky, 1995] Gorodnitsky, Irina F. and George, John S. and Rao, Bhaskar D. Neuromagnetic source imaging with FOCUSS: a recursive weighted minimum norm algorithm. *Electroencephalography and clinical Neurophysiology* 95, 231-251, 1995.

[Harrison, 1996] Harrison, Reid R. and Aine, Cheryl J. and Chen, Hai-wen and Edward R. Flynn, Edward R. and Huang, Mingxiong. Investigation of Methods for SpatioTemporal Neuromagnetic Source Localization, *Report: LA-UR-96-2042.*

[Huang, 1996] Huang, M. and Aine, C.J. and Supek, S. and Best, E. and Ranken, D. and Flynn, E.R. Multi-start Downhill Simplex Method for Spatio-temporal Source Localization in Magnetoencephalography, *Report LA-UR-96-2043.*

[Jin, 1993] Jin, Jianming. *The Finite Element Method in Electromagnetics* John Wiley and Sons, 1993.

[Makeig, 1994] Makeig S. and Jung T-P. and Bell A.J. and Ghahremani D. and Sejnowski T.J. Blind separation of event-related brain responses into Independent Components, *Proc. Natl. Acad. Sci.* USA, 1997.

[Mosher, 1992] Mosher, J.C. Lewis P.S. and Leahy R.M. Multiple dipole modeling and localization from spatio-temporal MEG data, *IEEE Trans. Biomed. Eng.* 39, 541-57, 1992.

[Nedler, 1965] Nedler, J.A. and Mead, R. A simplex method for function minimization, *Compt. J* 7, 308-313, 1965.

[Nunez, 1981] Nunez, P.L. *Electric Fields of The Brain,* New York: Oxford, 1981.

[Plonsey, 1995] Plonsey, R. Volume Conductor Theory, *The Biomedical Engineering Handbook* J.D. Bronzino, editor, 119-125, CRC Press, Boca Raton, 1995.

[Scherg, 1985] Scherg, M. and von Cramon, D. Two bilateral sources of the late AEP as identified by a spatio-temporal dipole model. *Electroenceph. clin. Neurophysiol.* 62, 290-299, 1985

[Schmidt, 1995] Schmidt, J.A. and Johnson, C.R. and Eason, J.C. and MacLeod, R.S. Applications of automatic mesh generation and adaptive methods in computational medicine, *Modeling, Mesh Generation, and Adaptive Methods for Partial Differential Equations* Babuska, I. *et al.*editors, Springer-Verlag, 367-390, 1995.

[Supek, 1993] Supek, S. and Aine, C.J. Simulation studies of multiple mipole neuromagnetic source localization: model order and limits of source resolution, *IEEE Trans. Biomed. Eng.* 40, 354-361, 1993

[Watson, 1981] Watson, D.F. Computing the n-dimensional Delaunay tesselation with applications to Voronoi polytopes, *Computer Journal* volume 24, number 2, 167-172, 1981.

[Wells, 1994] Wells, W.M. and Grimson, W.E.L. and Kikinis, R. and Jolesz, F.A. Statistical intensity correction and segmentation of MRI data, *Visualization in Biomedical Computing*, 13-24, 1994.

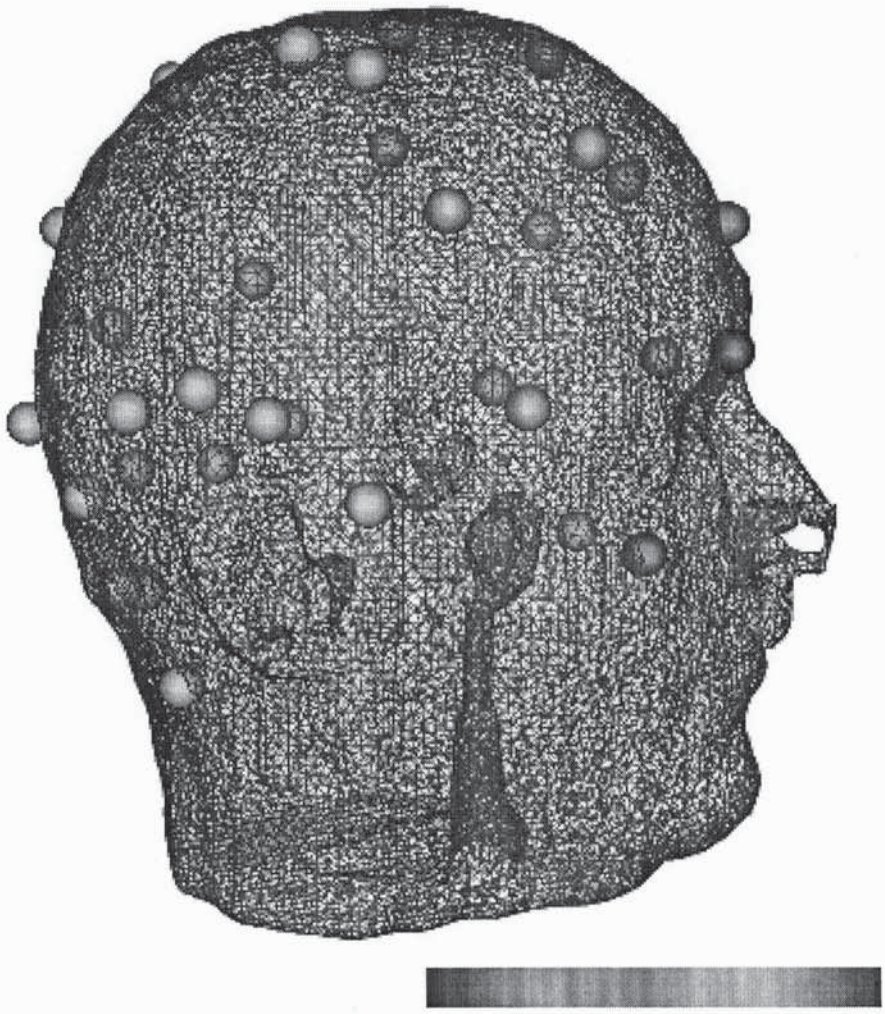

Figure 1: TRIANGULATED SCALP SURFACE WITH 32 ELECTRODES. THE ELECTRODES HAVE BEEN COLOR-MAPPED TO INDICATE ORDER: THEY ARE COLORED FROM BLUE TO RED AS THE CHANNEL NUMBER INCREASES.

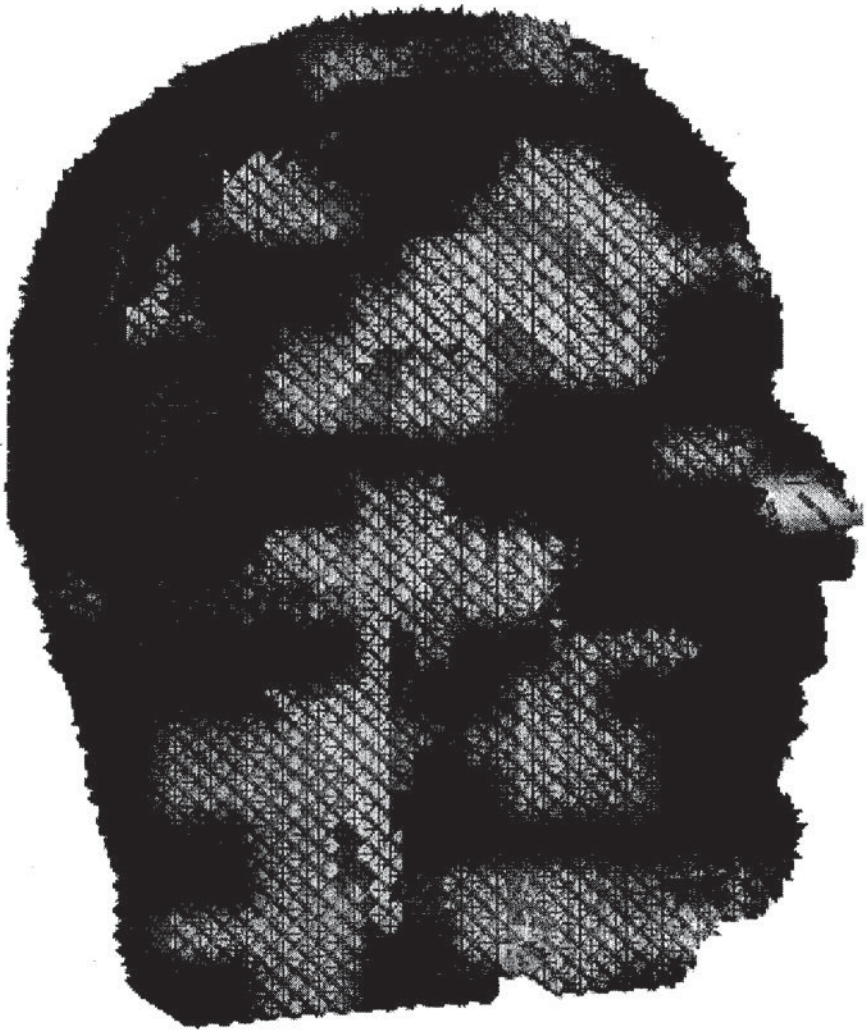

Figure 2: CUT-THROUGH OF THE TETRAHEDRAL MESH, WITH ELEMENTS COLORED ACCORDING TO CONDUCTIVITY CLASSIFICATION. GREEN ELEMENTS CORRESPOND TO SKIN, BLUE TO SKULL, YELLOW TO CEREBROSPINAL FLUID, PURPLE TO GRAY MATTER, AND BLUE TO WHITE MATTER.

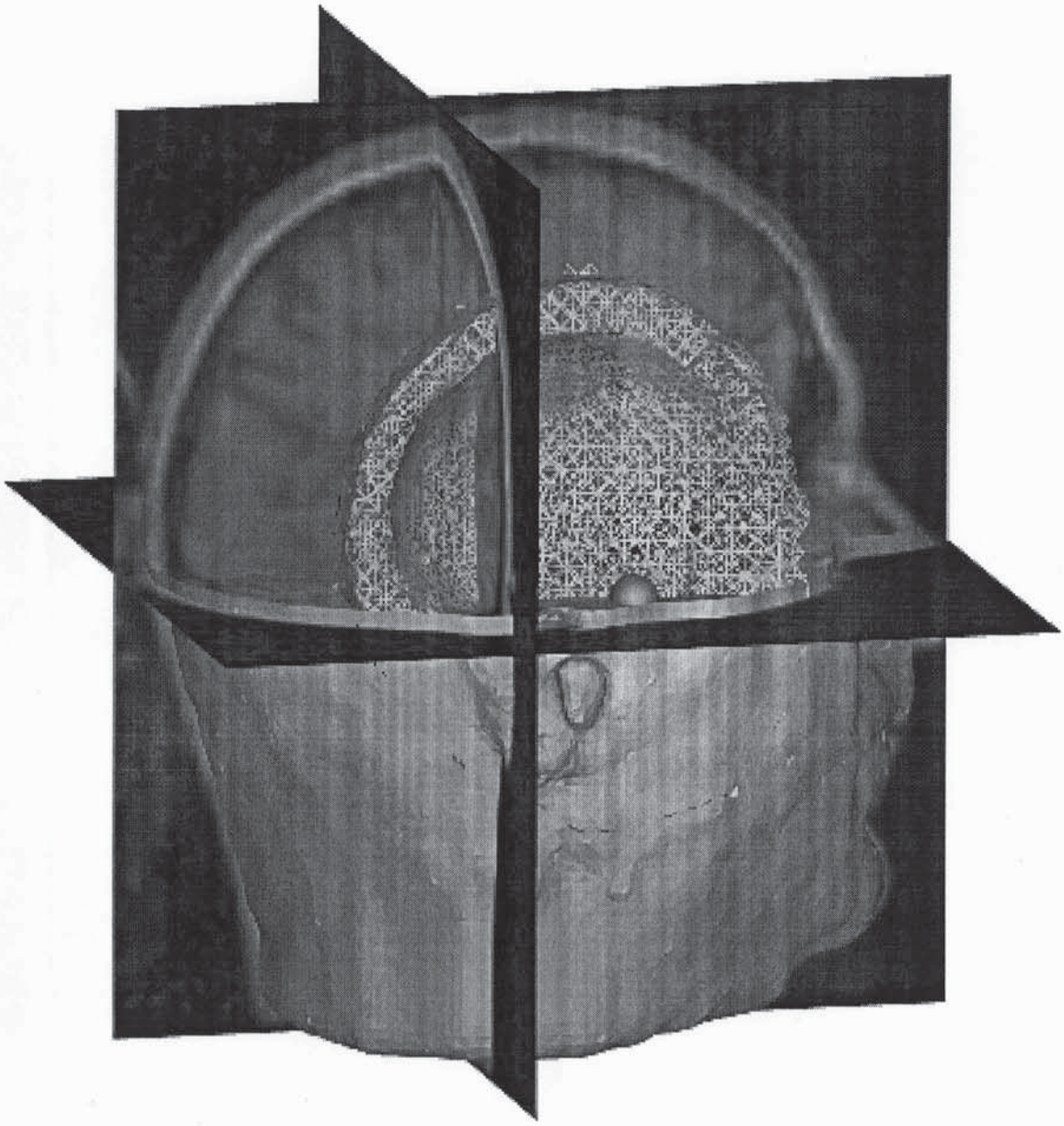

Figure 3: SOLUTION TO A SINGLE DIPOLE SOURCE FORWARD PROBLEM. THE UNDERLYING MODEL IS SHOWN IN THE MRI PLANES, THE DIPOLE SOURCE IS INDICATED WITH THE RED AND BLUE SPHERES, AND THE ELECTRIC FIELD IS VISUALIZED BY A CROPPED SCALP POTENTIAL MAPPING AND A WIRE-FRAME EQUIPOTENTIAL ISOSURFACE.

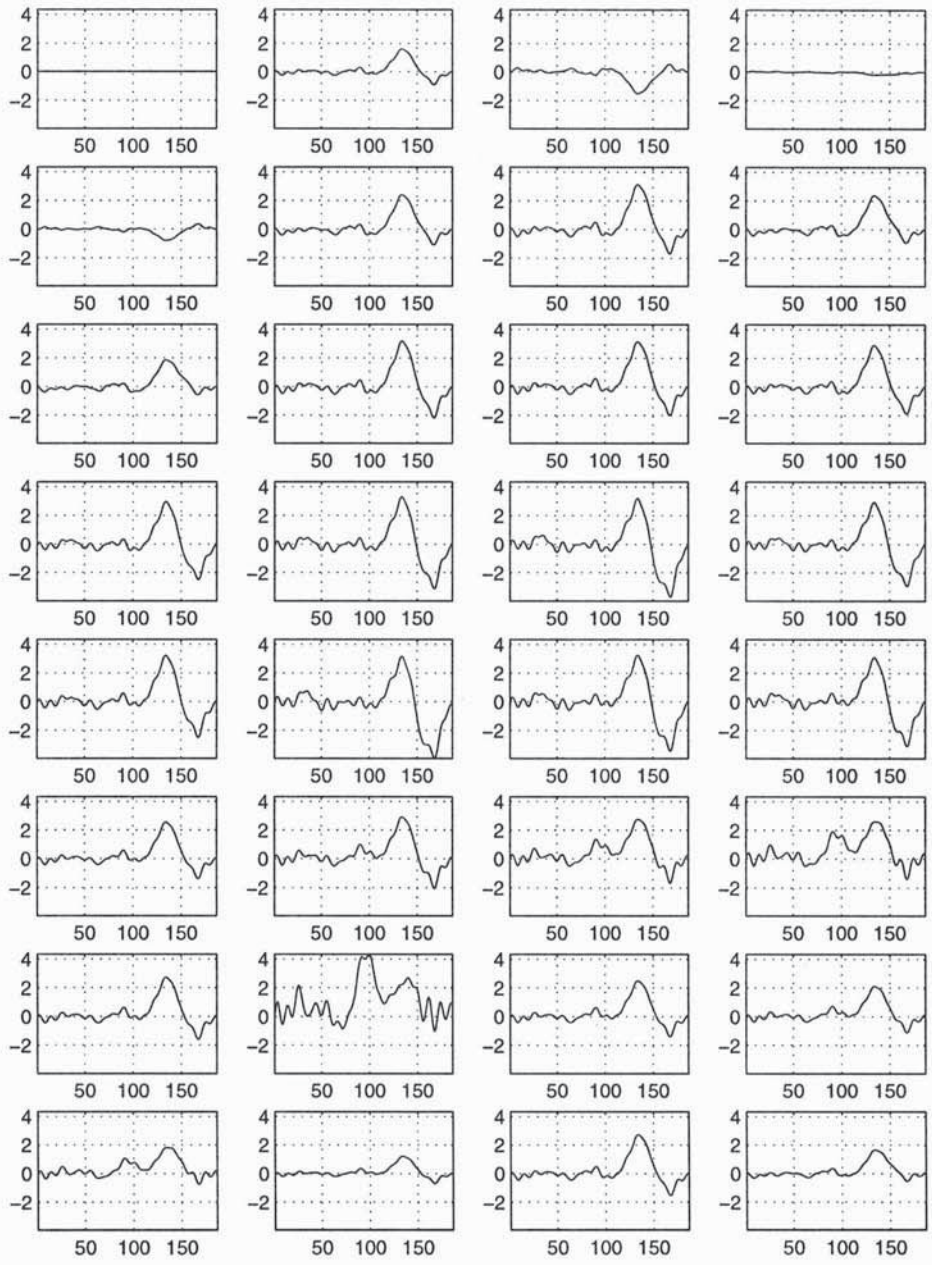

Figure 4: SIMULATED SCALP POTENTIAL DUE TO THREE DIPOLE SOURCES MAPPED ONTO 32 CHANNELS (ELECTRODES). CHANNELS ARE NUMBERED LEFT TO RIGHT, TOP TO BOTTOM. THE FIRST CHANNEL IS THE REFERENCE ELECTRODE. THESE SIGNALS ARE THE INPUT DATA FOR THE ICA ALGORITHM. THE LOCATIONS OF THESE 32 ELECTRODES ARE SHOWN IN FIGURE 1.

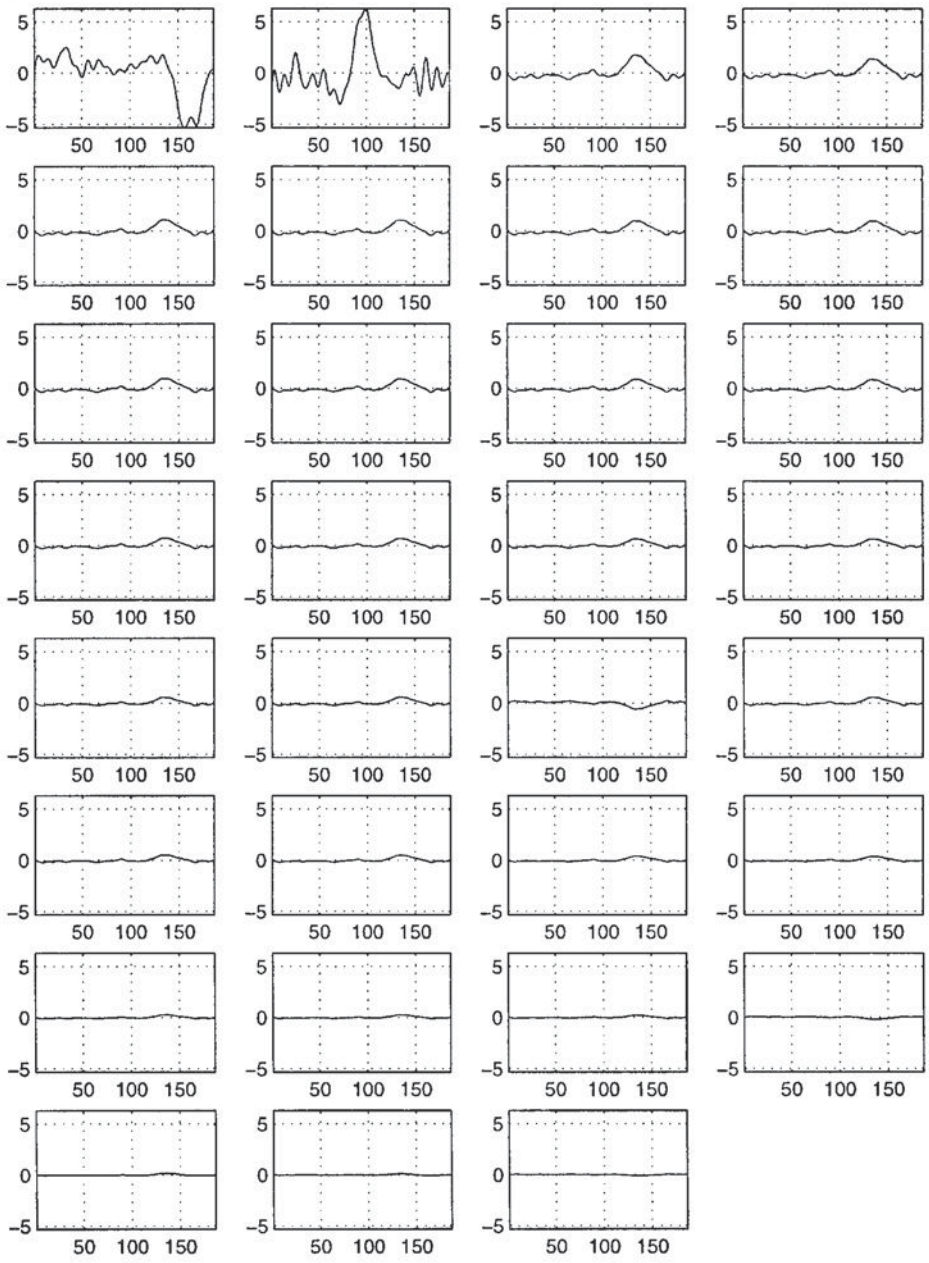

Figure 5: ICA ACTIVATION MAPS OBTAINED BY UNMIXING THE INPUT SIGNALS. WE OBSERVE THAT THERE ARE ONLY THREE INDEPENDENT PATTERNS, INDICATING THE PRESENCE OF ONLY THREE SEPARATE SIGNALS IN THE ORIGINAL DATA.

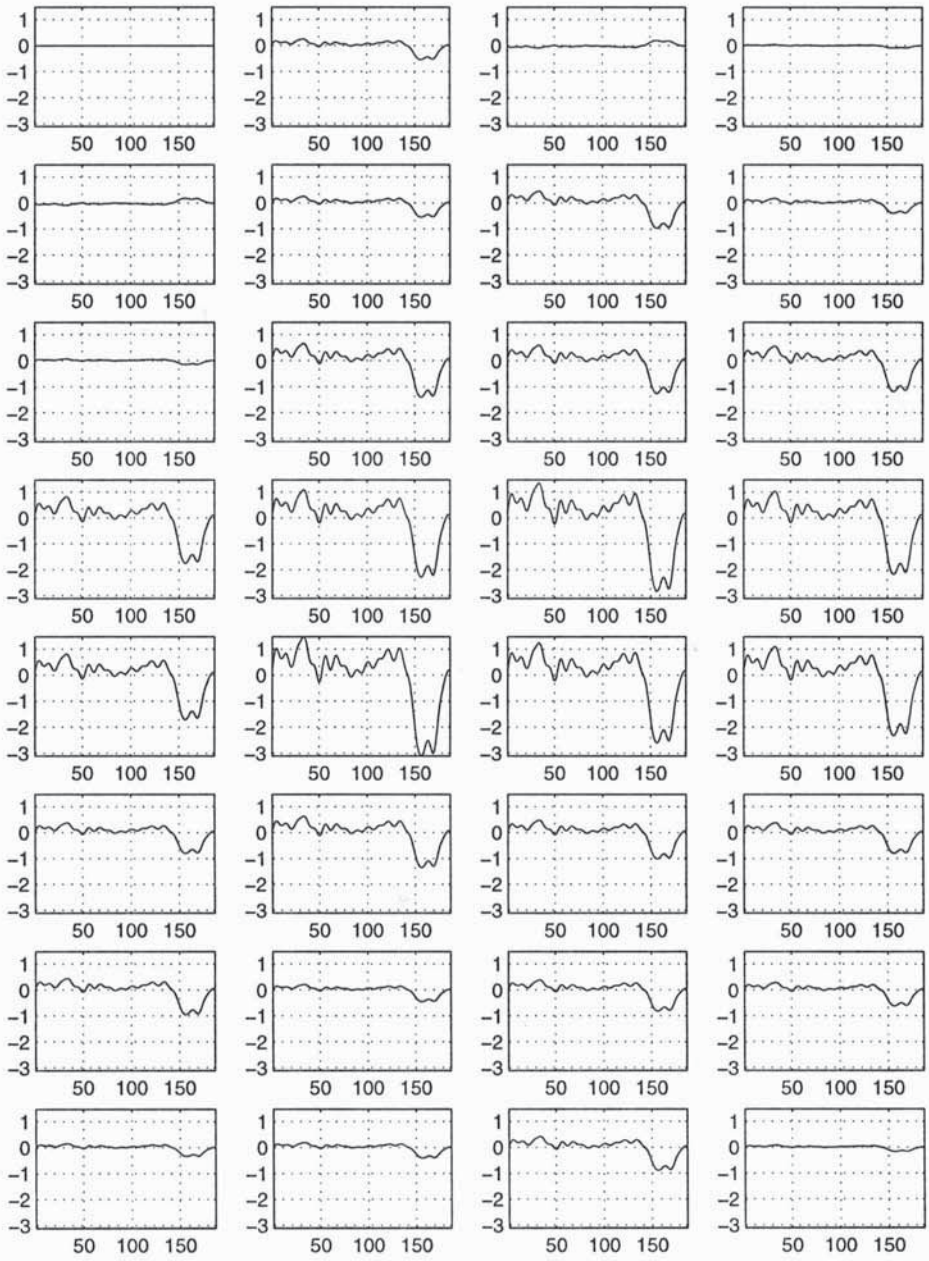

Figure 6: THE PROJECTION OF THE FIRST ACTIVATION MAP FROM FIGURE 5 ONTO THE 32 ELECTRODES.

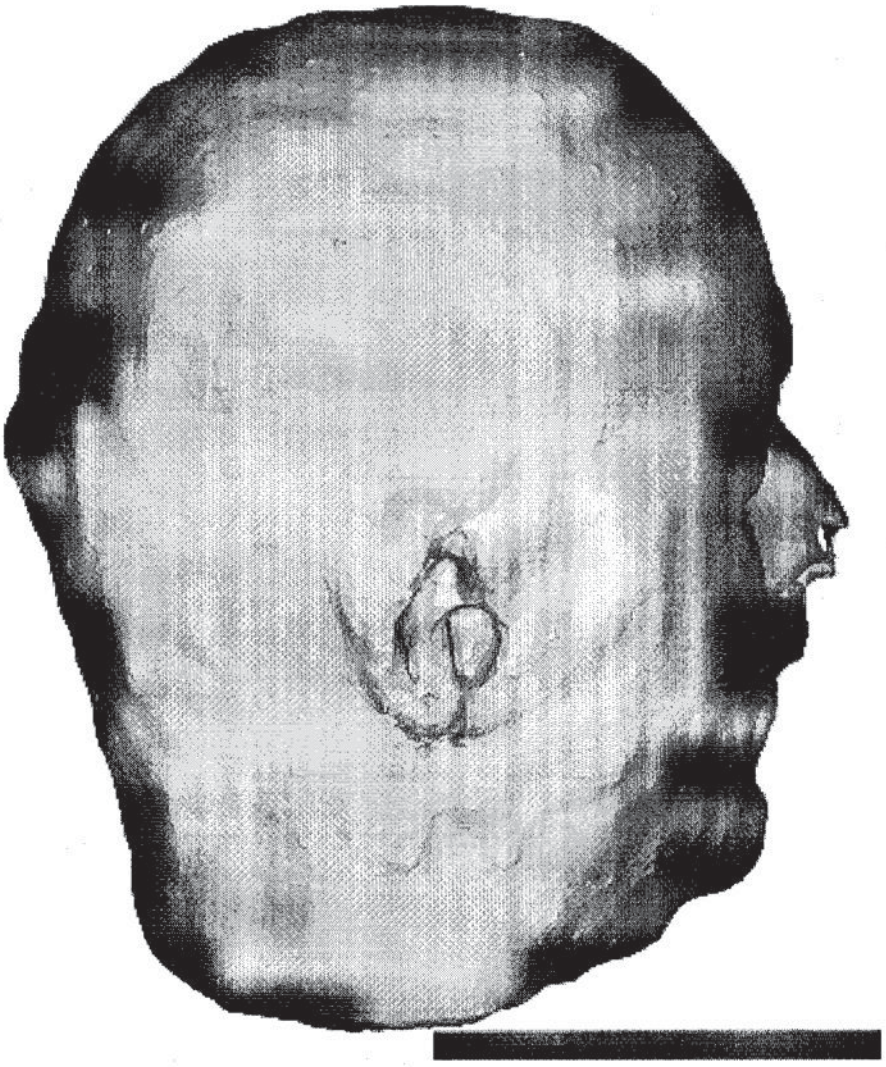

Figure 7: SCALP SURFACE POTENTIAL MAP DUE TO SEVERAL DIPOLES, CORRESPONDING TO TIME T=160MS FROM THE SIGNALS SHOWN IN FIGURE 4.

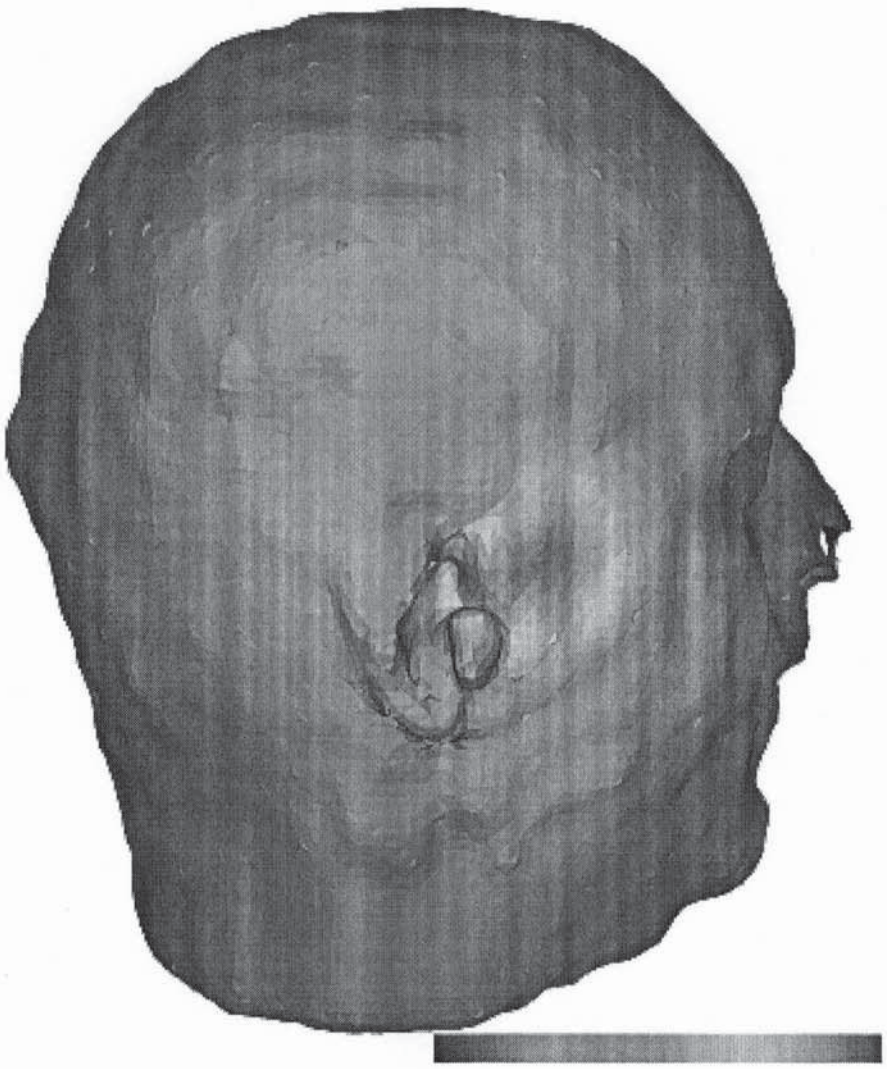

Figure 8: PROJECTION OF THE FIRST ICA COMPONENT ONTO THE 32 CHANNELS AT TIME T=160MS.